Effect of surface roughness, biofilm coverage and biofilm structure on the electrochemical efficiency of microbial cathodes

L. Pons, M.-L. Délia, A. Bergel *

Laboratoire de Génie Chimique, CNRS-Université de Toulouse, 4 allée Emile Monso, BP84234, 31030 Toulouse, France

A B S T R A C T

Biofilms of *Geobacter sulfurreducens* were formed under chronoamperometry at −0.5 V and −0.6 V vs. Ag/AgCl on stainless steel cathodes and tested for fumarate reduction. Increasing the surface roughness Ra from 2.0 μm to 4.0 μm increased currents by a factor of 1.6. The overall current density increased with biofilm coverage. When the current density was calculated with respect to the biofilm-coated area only, values up to 280 A/m^2 were derived. These values decreased with biofilm coverage and indicated that isolated cells or small colonies locally provide higher current density than dense colonies. Steel composition affected the current values because of differences in biofilm structure and electron transfer rates. Biofilms formed under polarisation revealed better electrochemical characteristics than biofilm developed at open circuit. This work opens up new guidelines for the design of microbial cathodes: a uniform carpet of isolated bacteria or small colonies should be targeted, avoiding the formation of large colonies.

1. Introduction

The technology of electrochemically active biofilms (EA biofilms) has been widely implemented to develop microbial fuel cells (Logan and Regan, 2006; Du et al., 2007; Lovley, 2008a; Franks and Nevin, 2010) but EA biofilms should also open up the development of many other novel processes in a wide variety of application sectors other than energy production (Di Lorenzo et al., 2009; Kim et al., 2009; Tront et al., 2008). A recent prospective review suggested that applications different from microbial fuel cells, including microbial electrosynthesis of fine chemicals, seemed more feasible and promising than MFCs in the near future (Pham et al., 2009). The oxidation of inexpensive organic matter coming from waste streams for the production of polyhydroxybutyrate or C3 and C4 chemicals has been evoked as a possible example. This review dealt with biofilm anodes only, but biofilm cathodes also can be envisaged as the source of new routes for bioelectrosynthesis. Indeed, there is a real economic interest in finding selective biocatalysts to lead to new electrosynthesis routes in biotechnology, as has been attempted for years with electro-enzymatic synthesis (Devaux-Basséguy et al., 1997; Ruinatscha et al., 2006; Kohlmann et al., 2008). Most recent papers have opened the range of applications of microbial cathodes to the extremely hot topic of CO_2 reduction to valuable organic compounds such as methane (Villano et al., 2010) or acetate and other organic compounds (Nevin et al., 2010). In this framework, it is of high importance to get an evaluation of the maximal current densities that microbial cathodes can provide and to find out engineering guidelines to improve microbial cathodes.

Geobacter sulfurreducens is known for its ability to reduce fumarate or Fe(III) oxides using solid electrodes as the sole source of electrons (Bond and Lovley, 2003; Esteve-Nunez et al., 2004; Gregory et al., 2004; Butler et al., 2006). Replacing the traditional graphite cathode by a stainless steel cathode has led to remarkably high current densities, up to 20 A/m^2 under polarisation at −0.6 V vs. Ag/AgCl (Dumas et al., 2008a). The purpose of the present work was to use the *G. sulfurreducens*-coated stainless steel cathodes as a model to progress in identifying parameters that affect the electron transfer rates at these interfaces. The effects of electrode material (austenitic 316L and superaustenitic 254SMO stainless steels), surface roughness and biofilm coverage on the current density were studied under constant potential polarisation at −0.5 V and −0.6 V vs. Ag/AgCl. The ultimate goal was to extract information to progress in designing optimal microbial stainless steel cathodes.

2. Methods

2.1. Media and growth conditions

G. sulfurreducens strain PCA (ATCC51573) was purchased from DSMZ (Deutsche Sammlung von Mikroorganismen und Zellkulturen). The growth medium contained per litre: 0.1 g KCl, 1.5 g NH_4Cl, 2.5 g $NaHCO_3$, 0.6 g NaH_2PO_4, 0.82 g sodium acetate, 8 g sodium fumarate, 10 mL Wolfe's vitamin solution (ATCC MD-VS) stored at −20 °C and 10 mL modified Wolfe's minerals (ATCC MD-TMS) stored at 4 °C. The medium without sodium fumarate,

* Corresponding author. Tel.: +33 0 5 34 32 36 73.
E-mail address: alain.bergel@ensiacet.fr (A. Bergel).

vitamins and minerals was first sterilised in bottles. The pH was adjusted to 6.8. After sterilisation, the medium was completed with the filtered (0.2 μm) stock solution of sodium fumarate. The growth procedure was made up of two successive steps. Firstly, *G. sulfurreducens* (10% v/v from an inoculum stored at −20 °C) was incubated at 30 °C for 80 h in the growth medium to obtain a final suspension with absorbance of 0.3 at 620 nm. Secondly, 5 mL of the suspension was inoculated in 45 mL of the same medium. The second incubation lasted 38 h and the final absorbance at 620 nm was 0.4.

2.2. Stainless steel electrodes

The working electrodes were made of 254SMO stainless steel (1 cm × 2.5 cm × 0.1 cm) or 316L stainless steel (2.5 cm × 2.5 cm × 0.1 cm) plates. 254SMO electrodes were always smooth (Ra around 0.1 μm) while different surface roughnesses of 316L were obtained by sand blasting. Each electrode was cleaned in stirred ethanol/acetone (50:50 v/v) solution for 20 min and rinsed in water for 30 min. 254SMO electrodes were also cleaned with fluoro-nitric acid (2 mL fluoridric acid, 20 mL nitric acid and 100 mL distilled water) for 20 min and rinsed in water for 60 min. Each electrode was drilled, tapped, and connected to a titanium wire to ensure the electrical connection. One face was coated with insulating resin (Resipoly Chrysor) to be sure of the electro-active surface area. When setting up the electrodes in the electrochemical reactor, care was taken to place the face that was used for the microbial settlement right in front of the auxiliary electrode.

2.3. Electrochemical reactors

The 0.5 L of electrochemical reactors was used with only one working electrode, while 2.5 L electrochemical reactors were implemented when three or four working electrodes were used together. The reactors contained, respectively 0.45 and 1.8 L of medium identical to the growth medium but without acetate. The medium was flushed with N_2–CO_2 (80–20%) for 24 h before the potential was applied. N_2–CO_2 bubbling was maintained at a lower flow rate during the experiments. The suspension of bacteria was injected into the reactors (10% v/v) after 24 h polarisation. The top of the 0.5 and 2.5 L reactors contained five and seven sampling ports, respectively, sealed with butyl stoppers. Ports were reserved for the auxiliary electrode, the reference electrode, the working electrode(s) and the gas outlet. The auxiliary electrode was a platinum grid (0.5 mm diameter wires, 90% Pt–10% Ir, Platecxis), which had been cleaned by heating to red-hot in a flame. The Ag/AgCl reference electrode was made of 1.5-mm-diameter silver wire dipped into HNO_3 solution and then immediately transferred into saturated KCl. The potential of the reference electrode was checked with a saturated calomel reference electrode (SCE) at the beginning and at the end of the experiment. In the conditions of the experiments, the Ag/AgCl reference had a potential of +0.313 V/SHE.

Chronoamperometry and cyclic voltammetry experiments were carried out with a multi-potentiostat (model VMP, software EC-Lab V9.20, Biologic SA). When several working electrodes were tested in the same 2.5 L-reactor, each was monitored independently by means of a N-STAT device (Bio-Logic SA). The current was recorded every 300 s. Cyclic voltammetries (CVs) were performed at 10 mV/s^1.

2.4. Microscopy method and statistical analysis

Topographic analysis of the surface of electrodes and average surface roughness (Ra) measurements were made using a white light interferometer, Zygo New View 100 OMP-0348K.

At the end of the experiments, the working electrodes were stained with a solution of 0.03% acridine orange (A6014, Sigma) for 10 min, rinsed with normal saline (9% NaCl) and air dried. Pictures were taken using a Carl Zeiss Axiotech 100 microscope equipped for epifluorescence with an HBO 50/ac mercury light source and Zeiss 09 filter (excitor AP 450-490, reflector FT 510, barrier filter LP 520) and a monochrome digital camera (Evolution VF). Images were processed with Image-Pro Plus V5 software.

The average biofilm coverage ratio (θ_A) was calculated from the numerical assessment of the coverage ratio (θ) of 40 pictures taken at different locations on the same electrode for smooth electrodes (up to Ra of 2.3 μm). Electrodes with roughness Ra above 2.3 μm gave blurred pictures because of parasite light coming from different planes, and no coverage ratio could be directly extracted. In these cases, composite pictures were made for each spot by taking 20 successive pictures at exactly the same location at different focal planes (*z*-distances perpendicular to the electrode surface). Each picture was cleared of the parasite light coming from the upper and lower planes (Optigrid system) and then all the pictures were piled together. Because of the time required to do this, the average biofilm coverage ratio θ_A was calculated from only five composite pictures which were constructed at different locations of the electrode surface.

3. Results and discussion

In each experiment, the electrochemical medium was similar to the standard culture medium used to grow the inoculum, but it did not contain the electron donor (acetate). The electrochemical medium contained the electron acceptor (50 mM fumarate) but no acetate was present in order to force the bacterial cells to use the electrode as the source of electrons. In these conditions, the current recorded under chronoamperometry corresponded to the electrochemical reduction of fumarate to succinate catalysed by the *G. sulfurreducens* biofilm that formed on the electrode surface, as already established (Bond and Lovley, 2003):

$$C_4H_4O_4 + 2H^+ + 2e^- \rightarrow C_4H_6O_4 \quad (1)$$

3.1. Influence of surface roughness and biofilm structure on 316L stainless steel cathodes

3.1.1. Correlation between global current density and surface roughness

Chronoamperometry was performed in a 2.5 L electrochemical reactor equipped with three 316L stainless steel working electrodes with different surface roughness. The control smooth electrode had an average roughness (Ra) of 0.1 μm, the two others had Ra of 2.3 and 4.0 μm. Electrodes were polarised at −0.6 V vs. Ag/AgCl and the reactor was inoculated with *G. sulfurreducens* one day after the beginning of chronoamperometry. It should be remarked that, depending on a lot of different parameters linked to the inoculum (time storage of the initial bacterial cells, age of the inoculum, time between the end of inoculum preparation and the electrochemical experiment, etc.) the electrochemical properties of the cells that develop on the electrode surface may vary from a reactor to another. With the objective of promoting the reproducibility of the microbial development, inoculum was prepared following a standardised two-step procedure that allowed the cell density to be strictly controlled at each step (see Section 2). Moreover, any cause of bias was avoided here by putting in the same reactor three working electrodes, which were addressed individually, in order for each electrode be exposed to exactly the same microbial conditions.

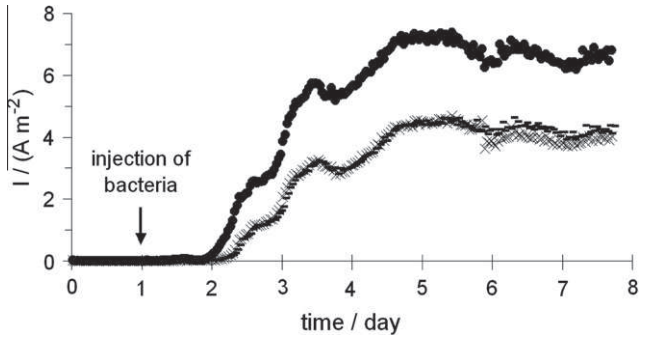

Fig. 1. Evolution of the current density during polarisation at −0.6 V vs Ag/AgCl on three 316L stainless steel electrodes with different surface roughness: control electrode Ra = 0.1 μm (-), Ra = 2.3 μm (×), and Ra = 4 μm (●).

Table 1
Maximal current density (J_{max}), average coverage ratios (θ_A) and intrinsic microbial current density ($J_{microbial}$) obtained in three independent experiments. Three or four individually addressed working 316L stainless steel electrodes with different surface roughness (Ra) were set up in each 2.5 L electrochemical reactor. Polarisation at −0.6 V vs. Ag/AgCl for EXP1 and −0.5 V vs. Ag/AgCl for EXP2 and EXP3.

Ra (μm)		0.1	2.3	2.4	3.7	4.0	6.1
EXP1 (−0.6 V)	J_{max} (A/m^2)	4	4			6.5	
	θ_A (%)	9	6			13	
	$J_{microbial}$ (A/m^2)	44	67			50	
EXP2 (−0.5 V)	J_{max} (A/m^2)	0.6	0.6			1	1
	θ_A (%)	12	9			12	22
	$J_{microbial}$ (A/m^2)	6.7	5.0			8.3	4.5
EXP3 (−0.5 V)	J_{max} (A/m^2)	1.5		3	3	2.5	
	θ_A (%)	2		11	9	9	
	$J_{microbial}$ (A/m^2)	75		27	33	11	

The current started to increase approximately 1 day after inoculation and reached an average maximal value (J_{max}) after 4 days. J_{max} was around 4 A/m^2 for the electrodes with the lowest average roughness (Ra = 0.1 and 2.3 μm), while the electrode with the highest roughness (Ra = 4.0 μm) reached 6.5 A/m^2 (Fig. 1 and Table 1 EXP1). The maximal current value remained stable for several days with weak circadian fluctuations as observed elsewhere for chronoamperometry with biofilm-coated anodes (Dulon et al. 2007). At the end of the chronoamperometry (day 8), the surface of each electrode was observed by epifluorescence microscopy. Pictures were taken at 40 different locations on the electrodes with the lowest Ra values (Ra = 0.1 and 2.3 μm). The 40 pictures were numerically treated to assess the biofilm coverage ratio θ for each picture, and the 40 values were then averaged to assess the global coverage ratio of the electrode θ_A. Average coverage ratios of 9 ± 2% and 6 ± 1%, were obtained for the control electrode (Ra = 0.1 μm) and the electrode with Ra of 2.3 μm, respectively (Fig. 2a and b). The high-roughness electrode (Ra = 4.0 μm) gave blurred pictures because the fluorescence coming from pits and valleys of the electrode surface could not be focused in a single focal plane. Consequently, the coverage ratio could not be extracted directly from these pictures. The photograph presented in Fig. 2c is a composite picture that resulted from a succession of 20 pictures taken at exactly the same location at different focal planes (see Section 2). Because of the time required to do this, only five different spots were investigated. The average coverage ratio was 13 ± 6%.

In this case, increasing the roughness from Ra = 0.1 to 2.3 μm did not have a significant effect on either current value or θ_A value. The electrode with Ra = 4.0 μm gave current 1.6 times higher than the control electrode, which approximately matched the 1.4-fold increase in the average coverage ratio. A direct correlation consequently appeared between maximal current and biofilm coverage.

Two other similar experiments with four individually addressed working electrodes were carried out under polarisation at −0.5 V vs. Ag/AgCl (EXP2 and EXP3 in Table 1). Whatever the value of the applied potential, the ratio of the maximum current density (J_{max}) provided by the electrode with Ra = 4.0 μm (present in each experiment) to that of the control electrode (Ra = 0.1 μm) was always around 1.6 to 1.7. It can be concluded from these 11 tests that the average surface roughness had a clear positive effect on the current above a threshold value, which was around 2.0 μm. Increasing the surface roughness no longer had an effect above values of 4.0 μm. The variation in current density corresponded to a homothetic variation in average biofilm coverage θ_A. These observations are consistent with some previous reports claiming that bacterial adhesion is favoured by surface roughness close to the size of the microbial cells (Flint et al., 2000).

3.1.2. Correlation between global current density and biofilm aspect

The increase of surface roughness corresponds to the accentuation of peaks and valleys on the electrode surface, which formally results in an augmentation of the area available for microbial settlement. A so-called "corrected surface area" was extracted from the topographic analysis, and represented the actual area that was available at the microscopic level for cell settlement. The corrected surface area was from 1.03 to 1.06 times the projected surface area for the electrodes with Ra from 2.3 to 4.0 μm, respectively. Consequently, the small increase in available surface area cannot explain the increase in biofilm coverage and current density. It must be concluded that roughness does not affect biofilm coverage by simply augmenting the geometric surface area available for bioadhesion, but really promotes bacterial settlement. Moreover, the different microscopy pictures showed that the increase in biofilm coverage was concomitant with the apparition of dense microbial clusters. The biofilm coverage did not increase uniformly on the whole surface but the highest coverage ratios corresponded to the formation of denser bacterial colonies. This is obvious in Fig. 2: pictures (a) and (b) show low coverage and mainly isolated bacterial cells, while pictures (c) and (d) show higher coverage and apparition of dense bacterial colonies.

3.1.3. Local current density or "intrinsic microbial current density"

We proposed here to assess the current density that the microbial cells really sustained locally ($J_{microbial}$) by dividing the whole current density by the surface area that was covered by the biofilm ($J_{microbial} = J_{max}/\theta_A$). The values of this "intrinsic microbial current density" are reported in Table 1. For a given experiment, this means for electrodes working in the same reactor i.e. in the same microbial conditions, $J_{microbial}$ was systematically lower for the highest biofilm coverage values. Thus the intrinsic electrochemical efficiency of the microbial cells decreased for the electrode surfaces that favoured higher biofilm coverage. Considering the structure of the biofilm, it can be concluded that microbial cells organised into denser colonies are less electrochemically efficient than isolated cells or small colonies. The current was linked to the biofilm coverage on the one hand, but also to the structure of the biofilm on the other hand. Summarizing, it can be concluded that:

- the global current density increased with biofilm coverage,
- biofilm coverage augmented with surface roughness in the range from 2 to 4 μm by forming widespread, dense microbial colonies,
- the intrinsic electrochemical efficiency of the microbial cells decreased in dense colonies.

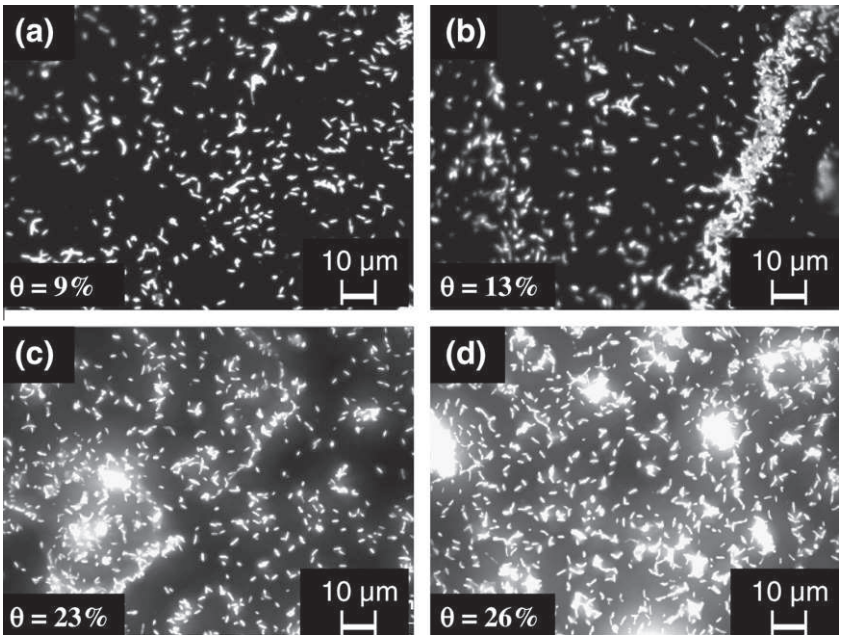

Fig. 2. Epifluorescence microscopy pictures of *G. sulfurreducens* biofilm on four 316L electrodes Ra = 0.1 µm (a), Ra = 2.3 µm (b), Ra = 4 µm (c) after 8 days polarisation at −0.6 V vs. Ag/AgCl for each electrode (EXP1), and Ra = 6.1 µm (d), after 15 days polarisation at −0.5 V vs. Ag/AgCl (EXP2). The biofilm coverage ratio (θ) is indicated on each picture.

3.2. Electrochemical activity and biofilm structure on 254SMO stainless steel cathodes

3.2.1. Chronoamperometry on 254SMO: correlation between global and local current density and biofilm structure

Four experiments were performed in four separate 0.5 L electrochemical reactors using 254SMO stainless steel smooth electrodes polarised at −0.6 V vs. Ag/AgCl. The evolution of the average current density calculated from the four experiments is reported in Fig. 3 (grey zone indicates the standard deviation). The current evolution was similar to the evolution observed with 316L electrodes but the current reached higher maximal values, on average around 12 A/m^2. This current value was of the same order of magnitude as the ones already reported with an identical *G. sulfurreducens* strain and similar 254SMO electrodes (Dumas et al., 2008a). This previous work that has used a single-step procedure for the inoculum preparation has resulted in large variation of the initial lag phase from 2 to 5 days. In the present work, the preparation of the strain following a well-controlled two-step procedure resulted in well-reproducible results and in a shorter initial lag phase. The good reproducibility induced here by the two-step preparation procedure was confirmed by similar experiments carried out in 2.5 L electrochemical reactors (data not shown).

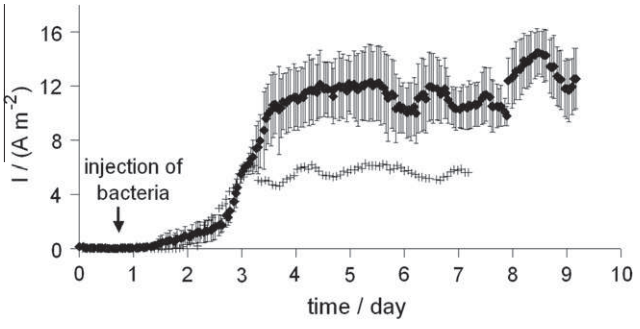

Fig. 3. Current density evolution on 254SMO stainless steel electrode polarised at −0.6 V vs Ag/AgCl. Black dots (♦) represent the average value and the grey zone represents the standard deviation obtained from four independent experiments. Crosses (+) represent the current density obtained on 254SMO electrode polarised at −0.5 V vs Ag/AgCl.

Epifluorescent microscopy pictures taken at the end of the experiments after 10 days polarisation showed heterogeneous microbial coverage made up of isolated microbial cells, small colonies and bigger bacterial colonies for the highest values of θ. Average coverage ratios θ_A (assessed through 40 pictures taken at different locations on each electrode) were 8 ± 2% and 5 ± 1% for the electrodes that sustained J_{max} of 13 and 14 A/m^2, respectively. The intrinsic microbial current densities ($J_{microbial}$) were 162 and 280 A/m^2 for θ_A values of 8% and 5%, respectively. These measurements on 254SMO electrodes confirmed that the intrinsic electrochemical efficiency of microbial cells decreased with biofilm coverage.

The distribution of the values of θ extracted from the 40 different pictures recorded on this electrode is represented in the form of histograms with span intervals of 5% (Fig. 4a). The histograms show that the 254SMO electrode surface was coated essentially with very small colonies, most of the pictures showing very low coverage ratios, between 0% and 5%. The remarkable capacity of *G. sulfurreducens* cells to catalyse the electrochemical reduction of fumarate should be emphasized here, as this electrode could sustain J_{max} = 14 A/m^2 with a visibly very low biofilm coverage. The $J_{microbial}$ value of 280 A/m^2 gives a better assessment of the electrocatalytic properties of the cells than the raw current. The same histogram presentation applied to a smooth 316L electrode that sustained 4 A/m^2 with θ_A = 9 ± 2% and $J_{microbial}$ = 44 A/m^2 showed that a higher number of microbial colonies had been able to develop in local dense colonies, most of the pictures giving coverage ratios between 5% and 10% (Fig. 4b). 254SMO stainless steel led to higher current density, and remarkably higher intrinsic microbial efficiency, than 316L stainless steel. This difference can be due to two convergent causes: as observed above, 316L seemed favouring the development of larger colonies, which are intrinsically less efficient. On the other hand, the nature of the material has a direct effect on the electron transfer rate. Electrochemical investigations looking at the semi-conductive properties of the

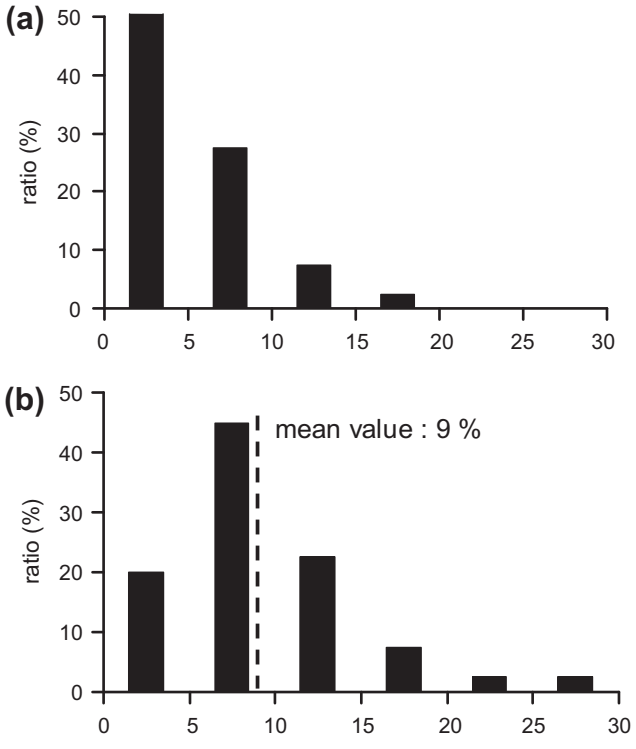

Fig. 4. Distribution of the θ values obtained from epifluorescence microscopy pictures on 40 different spots for each electrode. *G. sulfurreducens* biofilms grown 10 days with polarisation at −0.6 V vs. Ag/AgCl on 254SMO stainless steel (a), and 316L stainless steel (b).

passive layers indicated that 254SMO is more favourable to cathodic electron transfer than 316L (data not shown, to be published).

3.2.2. Electrochemical kinetics

Cyclic voltammograms were recorded after 24 h of polarisation i.e. just before inoculation of the reactor, and at the end of the experiment after 10 days polarisation at −0.6 V vs. Ag/AgCl. Before inoculation, no current production occurred in the potential range (Fig. 5a). At the end of the experiment, in the presence of a 10-days old biofilm, the reduction process started around −0.27 V vs. Ag/AgCl and exhibited an exponential shaped curve over the whole range of potentials scanned, suggesting that the reduction was controlled by electrochemical-like kinetics (Fig. 5b). A low oxidation reaction appeared above −0.27 V vs. Ag/AgCl. To characterise the reduction kinetics, a 254SMO electrode was first polarised at −0.6 V vs Ag/AgCl until the current density was stable at its maximal value. Different increasing potential values were then applied successively for a few hours so as to obtain stable values of current at each potential step. The current densities plotted as a function of the applied potential in logarithmic scale indicated fair Tafel kinetics (Fig. 5c and d). Placing the *x*-axis at the redox potential of the fumarate/succinate couple (−0.28 V vs. Ag/AgCl) gave an exchange current density J_0 of 5.3 A/m^2. Assuming that two electrons were exchanged per molecule of fumarate (Eq. (1)), the slope of the curve gave a charge transfer coefficient α of 0.43. The high value of J_0 confirms the capacity of the biofilm to exchange electrons with stainless steel; the value of α, close to the basic 0.5 value, confirms the control by a pure electrochemical kinetics. An identical electrochemical analysis applied to the same system has given in a previous report J_0 = 2.6 A/m^2 and α = 0.03 (Dumas et al., 2008a). In the previous report the biofilm was formed during 15 days with no applied potential (open circuit), while it was formed here by 10 days constant polarisation at −0.6 V vs. Ag/AgCl. The low value of α obtained in the previous study has been attributed to a possible effect of the metal oxides that constitute the surface layer of stainless steel. Two hypotheses can be proposed to explain the higher efficiency of the biofilm-electrode interface obtained here: either forming biofilm under constant polarisation increased the efficiency of the microbial catalysis, and/or it reduced metal oxides resulting in better electrochemical efficiency of the material. Whatever the fine explanation, forming *G. sulfurreducens* biofilm under polarisation was shown here to improve the electrochemical characteristics of the biocathode.

Only a very weak oxidation current was detected in the range −0.2 and −0.1 V vs Ag/AgCl during the successive electrolyses. The oxidation phenomenon observed on the CV (Fig. 5b) was consequently a transient phenomenon, which was not sustained by a steady-state oxidation process. Such a fast transient electron exchange has already been observed with *G. sulfurreducens* biofilms that catalysed the oxidation of acetate (Parot et al., 2008). It has been attributed to fast electron exchanges between the electrode and the redox systems of the cells that may act as so-called "electron sponge" (Dumas et al., 2008b). This assumption has been strengthened by discovering that *Geobacter* cells contain a large amount of iron molecules (c-type cytochromes) in their periplasm and outer membrane that can serve for electron storage (Esteve-Nunez et al., 2008; Lovley, 2008b).

Finally, a biofilm was formed similarly on a 254SMO electrode but under polarisation at −0.5 V vs Ag/AgCl, instead of −0.6 V in the previous experiment. A traditional current-time curve as reported in Fig. 3 was observed. The initial lag time was not significantly affected by the value of the polarisation potential. The coverage ratio obtained after 5 days of polarisation, θ_A = 10 ± 2%, was of the same order of magnitude as the values obtained previously at −0.6 V but the maximal current around 5.5 A/m^2 was lower, in accordance with the kinetics observed by cyclic voltammetry. Biofilms showed similar coverage ratio, similar structure and similar electrochemical behaviour when formed under −0.5 and −0.6 V vs. Ag/AgCl, although the current provided was significantly different. Consequently, in this range of potential values, the development of the biofilm was disconnected from the electrochemical reaction of fumarate reduction: in the range −0.5 and −0.6 V vs. Ag/AgCl biofilm formation was not affected by the potential, while fumarate reduction followed a classical Tafel law.

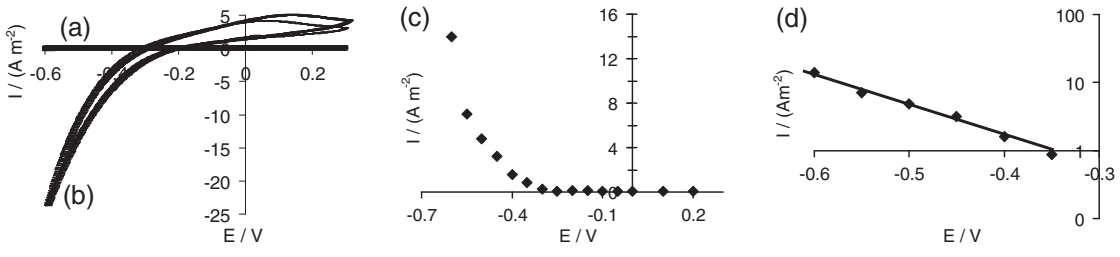

Fig. 5. Cyclic voltammograms at 10 mV/s on 254SMO stainless steel electrodes before the injection of bacteria (a), and after 10 days polarisation at −0.6 V vs. Ag/AgCl (b). Stable current density at different potential on a 254SMO stainless steel electrode previously polarised at −0.6 V vs Ag/AgCl for 10 days (c), and same current density values plotted on logarithmic scale (d).

3.3. Guidelines for engineering

Considering the data obtained here, we can propose a set of general guidelines that should lead to progress in optimising microbial cathodes. First, an average surface roughness Ra of around 4.0 μm is the best choice because higher values do not have a greater effect. The overall current density increased with biofilm coverage, so the most complete microbial settlement possible must be a logical target. Nevertheless, the intrinsic microbial current density decreased with biofilm coverage, which means that the microbial cells locally gave less and less current when the biofilm developed on the electrode surface. The structure of biofilms had a drastic effect on the current provided by the microbial cathodes. Isolated cells and small colonies locally provided higher current density than dense colonies. One of the main conclusions of the work is that the optimal biofilm structure is a dense carpet of small microbial colonies. Operating conditions for biofilm formation should now be defined in the aim of favouring such a final structure and avoiding the formation of large-size colonies. The composition of the steel affects the current density values by inducing differences in biofilm structure. 254SMO exhibited a better capability to develop efficient electroactive biofilms than 316L. Different electron transfer rates were also noted for the two types of stainless steel used here but this topic was not developed. Finally, biofilms should be formed under polarisation rather than at open circuit. These guidelines are certainly valid for the design of optimal cathodes and probably for optimal anodes provided the biofilms achieve a similar electron transfer mechanism to those implemented by the *G. sulfurreducens* biofilms used here i.e. direct electron transfer through membrane-bound redox compounds (cytochromes). However, some conclusions might be different if different electron transfer mechanisms were involved, such as soluble redox mediators for example.

4. Conclusions

The global current density increased but the intrinsic microbial current density decreased with biofilm coverage. This phenomenon was due to the formation of dense microbial colonies that locally provided lower current densities than isolated bacteria or small colonies. Calculations showed that current densities up to 280 A/m^2 could be achieved locally by microbial electro-catalysis. This order of magnitude can be now considered as a realistic objective for microbial cathodes. The optimal microbial settlement that must be targeted is a uniform carpet of multiple isolated bacteria or small colonies, avoiding the formation of large colonies.

Acknowledgements

This work was part of the "ANR non thématique" project "Bacteriopile" (ANR-05-PNT05-3_ 43343). The authors are grateful to V. Baylac (CIRIMAT – Toulouse) for help with the roughness measurements, L. Etcheverry (LGC – Toulouse) for efficient technical help, P. Floquet (LGC – Toulouse) for his kind contribution to the statistical analysis, Ugine & ALZ for providing rough 316L stainless steel samples, and CEA-Saclay for providing 254SMO samples.

References

Bond, D.R., Lovley, D.R., 2003. Electricity production by *Geobacter sulfurreducens* attached to electrodes. Appl. Environ. Microbiol. 69, 1548–1555.

Butler, J.E., Glaven, R.H., Esteve-Nunez, A., Nunez, C., Shelobolina, E.S., Bond, D.R., Lovley, D.R., 2006. Genetic characterization of a single bifunctional enzyme for fumarate reduction and succinate oxidation in *Geobacter sulfurreducens* and engineering of fumarate reduction in *Geobacter metallireducens*. J. Bacteriol. 188, 450–455.

Devaux-Basséguy, R., Bergel, A., Comtat, M., 1997. Potential applications of NAD(P)-dependent oxidoreductases in synthesis: a survey. Enzyme Microb. Technol. 20, 248–258.

Di Lorenzo, M., Curtis, T.P., Head, I.M., Scott, K., 2009. A single chamber microbial fuel cell as a biosensor for wastewaters. Water Res. 43, 3145–3154.

Du, Z., Li, H., Gu, T., 2007. A state of the art review on microbial fuel cells: a promising technology for wastewater treatment and bioenergy. Biotechnol. Adv. 25, 464–482.

Dulon, S., Parot, S., Délia, M., Bergel, A., 2007. Electroactive biofilms: new means for electrochemistry. J. Appl. Electrochem. 37, 173–179.

Dumas, C., Basseguy, R., Bergel, A., 2008a. Microbial electrocatalysis with *Geobacter sulfurreducens* biofilm on stainless steel cathodes. Electrochim. Acta 53, 2494–2500.

Dumas, C., Basseguy, R., Bergel, A., 2008b. Electrochemical activity of *Geobacter sulfurreducens* biofilms on stainless steel anodes. Electrochim. Acta 53, 5235–5241.

Esteve-Nunez, A., Nunez, C., Lovley, D.R., 2004. Preferential reduction of Fe(III) over fumarate by *Geobacter sulfurreducens*. J. Bacteriol. 186, 2897–2899.

Esteve-Nunez, A., Sosnik, J., Visconti, P., Lovley, D.R., 2008. Fluorescent properties of c-type cytochromes reveal their potential role as an extracytoplasmic electrfon sink in *Geobacter sulfurreducens*. Environ. Microbiol. 10, 497–505.

Flint, S.H., Brooks, J.D., Bremer, P.J., 2000. Properties of the stainless steel substrate, influencing the adhesion of thermo-resistant streptococci. J. Food Eng. 43, 235–242.

Franks, A.E., Nevin, K.P., 2010. Microbial fuel cells, a current review. Energies 3, 899–919.

Gregory, K.B., Bond, D.R., Lovley, D.R., 2004. Graphite electrodes as electron donors for anaerobic respiration. Environ. Microbiol. 6, 596–604.

Kim, M., Hyun, M.S., Gadd, G.M., Kim, G.T., Lee, S.J., Kim, H.J., 2009. Membrane-electrode assembly enhances performance of a microbial fuel cell type biological oxygen demand sensor. Environ. Technol. 30, 329–336.

Kohlmann, C., Maerkle, W., Luetz, S., 2008. Electroenzymatic synthesis. J. Mol. Catal. 51, 57–72.

Logan, B.E., Regan, J.M., 2006. Electricity-producing bacterial communities in microbial fuel cells. Trends Microbiol. 14, 512–518.

Lovley, D.R., 2008a. The microbe electric: conversion of organic matter to electricity. Curr. Opin. Biotechnol. 19, 564–571.

Lovley, D.R., 2008b. Extracellular electron transfer: wires, capacitors, iron lungs, and more. Geobiology 6, 225.

Nevin, K.P., Woodard, T.L., Franks, A.E., Summers, Z.M., Lovley, D.R., 2010. Microbial electrosynthesis: feeding microbes electricity to convert carbon dioxide and water to multicarbon extracellular organic compounds. MBio 1 (2), e00103–e00110.

Parot, S., Délia, M.-L., Bergel, A., 2008. Acetate to enhance electrochemical activity of biofilms from garden compost. Electrochim. Acta 53, 2737–2742.

Pham, T.H., Aelterman, P., Verstraete, W., 2009. Bioanode performances in bioelectrochemical systems: recent improvements and prospects. Trends Biotechnol. 27, 168–178.

Ruinatscha, R., Hoellrigl, V., Otto, K., Schmid, A., 2006. Productivity of selective electroenzymatic reduction and oxidation reactions: theoretical and practical considerations. Adv. Synth. Catal. 348, 2015–2026.

Tront, J.M., Fortnerb, J.D., Plötzea, M., Hughesb, J.B., Puzrina, A.M., 2008. Microbial fuel cell biosensor for *in situ* assessment of microbial activity. Biosens. Bioelectron. 24, 586–590.

Villano, M., Aulenta, F., Ciucci, C., Ferri, T., Giuliano, A., Majone, M., 2010. Bioelectrochemical reduction of CO_2 to CH_4 via direct and indirect extracellular electron transfer by a hydrogenophilic methanogenic culture. Bioresour. Technol. 101, 3085–3090.